

## Controlling relative polymorph stability in soft porous crystals with a barostat

Nathan A. Mahynski and Vincent K. Shen

Citation: *The Journal of Chemical Physics* **146**, 224706 (2017); doi: 10.1063/1.4983616

View online: <http://dx.doi.org/10.1063/1.4983616>

View Table of Contents: <http://aip.scitation.org/toc/jcp/146/22>

Published by the [American Institute of Physics](#)

---

---

**COMPLETELY**

**REDESIGNED!**



**PHYSICS  
TODAY**

*Physics Today* Buyer's Guide  
Search with a purpose.

# Controlling relative polymorph stability in soft porous crystals with a barostat

Nathan A. Mahynski<sup>a)</sup> and Vincent K. Shen

*Chemical Sciences Division, National Institute of Standards and Technology, Gaithersburg, Maryland 20899-8320, USA*

(Received 2 March 2017; accepted 2 May 2017; published online 14 June 2017)

We use Monte Carlo simulations to investigate the thermodynamic behavior of soft porous crystal (SPC) adsorbents under the influence of an external barostat. We consider SPCs that naturally exhibit polymorphism between crystal forms of two distinct pore sizes. In the absence of barostatting, these crystals may be naturally divided into two categories depending on their response to stress applied by the adsorbate fluid: those which macroscopically deform and change the volume of their unit cell (“breathing”) and those which instead undergo internal rearrangements that change the adsorbate-accessible volume without modifying the unit cell volume (“gate-opening”). When breathing SPCs have a constant external pressure applied, in addition to the thermodynamic pressure of the adsorbate fluid, we find that the free energy difference between the crystal polymorphs is shifted by a constant amount over the entire course of adsorption. Thus, their relative stability may be easily controlled by the barostat. However, when the crystal is held at a fixed overall pressure, changes to the relative stability of the polymorphs tend to be more complex. We demonstrate a thermodynamic analogy between breathing SPCs held at a fixed pressure and macroscopically rigid gate-opening ones which explains this behavior. Furthermore, we illustrate how this implies that external mechanical forces may be employed to tune the effective free energy profile of an empty SPC, which may open new avenues to engineer the thermodynamic properties of these polymorphic adsorbents, such as selectivity. [<http://dx.doi.org/10.1063/1.4983616>]

## I. INTRODUCTION

Soft porous crystals (SPCs) are a subset of metal-organic framework materials which can undergo large-scale reversible deformation due to imposed stresses.<sup>1–4</sup> These stresses may be a result of externally applied mechanical pressure or interactions with an adsorbing fluid, both of which can induce a thermodynamic transition from one crystal form to another. Broadly speaking, there are two classes of SPCs based on the nature of the transformation that occurs. The imposed stress may cause the organic linkers in the SPC to, e.g., rotate or displace, which changes the internally accessible volume to an adsorbate fluid but does not change the SPC’s unit cell volume. Alternatively, the SPC may be macroscopically deformed in a manner which does lead to changes in this volume. Perhaps the most common examples of the former are “gate-opening” materials such as zeolitic imidazolate framework (ZIF)-8 and members of the ELM family.<sup>3,5,6</sup> The latter process instead leads to “breathing” SPCs such as MIL-47(V) and MIL-53; these SPCs contain a “wine-rack” motif that expands and contracts in response to stress, thus changing the unit cell volume while maintaining mechanical integrity.<sup>7–10</sup>

This polymorphism between well-defined “narrow pore” (NP) and “large pore” (LP) forms is tied to the free energy landscape,  $F_s(h)$ , of the SPC which can exhibit multiple minima as a function of pore size,  $h$ , even when no adsorbate is

present. The specific shape of this landscape is determined by the organic linkers between metal centers in the SPC and may be engineered simply by changing the chemistry of these linkers.<sup>10,11</sup> SPCs are expected to have not only mechanical utility as nanosprings and dampers<sup>10</sup> but are also candidates for performing efficient selective chemical separations,<sup>12–15</sup> catalysis,<sup>16</sup> and as pharmaceutical delivery systems.<sup>17</sup> Consequently, both theoretical<sup>7,13,18</sup> and computational investigations<sup>11,15,19</sup> have been undertaken to understand the thermodynamic stability of these polymorphs.

Recently, we used a flat-histogram Monte Carlo approach to systematically investigate the effects of tuning  $F_s(h)$  in a model slit-pore adsorbent using free energy profiles representative of those found in SPCs.<sup>10,15</sup> This approach allows us to easily investigate the thermodynamics of both stable and metastable states of the combined fluid-crystal system for multicomponent adsorbates. In this work, we expand upon that investigation by examining the impact of modifying the total pressure applied on the SPC via mechanical means. We use this simple, but informative model to explore the consequences of barometric control over characteristic properties of a SPC, such as its selectivity. A recent theoretical investigation has suggested a practical route to achieving barometric control by casting SPCs into composites, e.g., core-shell particles, where the elasticity of a surrounding non-adsorbing matrix can be used to dampen SPC deformations.<sup>20</sup> However, to our knowledge this has neither been tested with simulations nor explored systematically in the context of selective separation of multicomponent fluids.

<sup>a)</sup>Electronic mail: [nathan.mahynski@nist.gov](mailto:nathan.mahynski@nist.gov)

We and others have previously illustrated two thermodynamic ensembles which are representative of gate-opening and breathing materials, which we refer to as the “grand canonical pore” and “osmotic pore” ensembles, respectively.<sup>11,15,19,21</sup> Here we specifically consider the latter subject to two conditions: one, where a constant additive pressure is placed on a breathing SPC over the course of adsorption, and two, where the SPC is instead held at a fixed overall pressure. We illustrate how these conditions can be used to tune the relative stability of the different crystal polymorphs for different characteristic  $F_s(h)$  profiles. Furthermore, for a model slit-pore system, we demonstrate the thermodynamic analogy between breathing materials held at a constant pressure and unconstrained gate-opening materials; this ultimately implies that tuning the mechanical forces applied to a macroscopically deformable SPC is equivalent to changing its inherent  $F_s(h)$  profile, which suggests a way to tune the SPC’s effective thermodynamic properties via external means. In this work, we focus on a supercritical, binary, size-asymmetric adsorbate mixture as an illustrative example of these concepts.

This paper is organized as follows. In Section II we discuss the model system and computational methodology employed here to systematically investigate breathing SPCs with different characteristic free energy profiles. Section III presents the consequences of imposing different pressure conditions (additive vs. fixed) on these adsorbents, and the effects this has on their selectivity. Conclusions and some future outlook are presented in Section IV.

## II. METHODS

In this work, we modeled a SPC as a single slit-pore in a three-dimensional rectilinear simulation box. The pore was periodic in the  $x$  and  $y$  directions, but non-periodic in  $z$ , which was bounded by the walls of the slit-pore. Our adsorbate was a binary fluid mixture that interacted with itself via a square-well potential given by

$$U_{i,j}(r) = \begin{cases} \infty & r \leq \sigma_{i,j} \\ -\epsilon_{i,j} & \sigma_{i,j} < r \leq \lambda_{i,j}\sigma_{i,j}, \\ 0 & \lambda_{i,j}\sigma_{i,j} < r \end{cases} \quad (1)$$

where  $r$  is the interparticle separation for a particle of species  $i$  and a particle of species  $j$ , and  $\epsilon_{i,j}$  is their pairwise interaction energy. These fluid particles also interacted with the walls of the slit-pore via a square-well potential, such that

$$U_{i,w}(z) = \begin{cases} \infty & |z - h_z| \leq \sigma_{i,i}/2 \\ -\epsilon_{i,w} & \sigma_{i,i}/2 < |z - h_z| \leq \lambda_{i,w}\sigma_{i,i}, \\ 0 & \lambda_{i,w}\sigma_{i,i} < |z - h_z| \end{cases} \quad (2)$$

where  $h_z$  indicates the wall bounds, one at  $z = h/2$  and another at  $z = -h/2$ . Following our previous work,<sup>15</sup> the parameters for

TABLE I. Pairwise, square-well interaction parameters for the binary fluid investigated.

$i$	$j$	$\epsilon_{i,j}$	$\sigma_{i,j}$	$\lambda_{i,j}$
1	1	1.20	1.50	1.33
1	2	1.10	1.25	1.40
2	2	1.00	1.00	1.50

TABLE II. Square-well interaction parameters for each species with the slit-pore walls.

Case	$\lambda_{1,w}$	$\epsilon_{1,w}$	$\lambda_{2,w}$	$\epsilon_{2,w}$
I	1.50	2.50	1.50	2.50
II	1.50	5.00	1.50	2.50
III	1.00	2.50	1.50	2.50
IV	1.50	2.50	1.50	5.00

the fluid-fluid and fluid-wall interactions are given in Tables I and II, respectively. The temperature for all simulations was  $T^* \equiv k_B T / \epsilon_{2,2} = 1.35$  ( $k_B$  is Boltzmann’s constant), which is supercritical for this mixture.<sup>15</sup> All lengths, energies, and quantities derived from these are reported in units of  $\sigma_{2,2}$  and  $\epsilon_{2,2}$  unless otherwise stated. We performed grand canonical Wang-Landau Transition Matrix Monte Carlo (WL-TMMC) simulations of the bulk binary fluid system at discrete values of  $\mu_1$  and  $\Delta\mu_2 \equiv \mu_2 - \mu_1$ . Here  $\mu_i$  refers to the chemical potential of species  $i$ . This allows us to reconstruct a curve of  $(\mu_1, \mu_2)$  along which the bulk fluid’s composition is fixed as its pressure is increased; this curve defines the conditions for which the pore is in equilibrium with the bulk fluid at a given adsorbate fluid pressure,  $P_f$ , and composition.<sup>15</sup>

These simulations were also repeated in confinement at different fixed pore widths,  $h$ . As described elsewhere,<sup>15,19</sup> this flat-histogram approach allows us to use these simulations to reconstruct the joint macrostate probability distribution,  $\Pi(h, N_{\text{tot}})$ , for each ensemble along arbitrary bulk isopleths (constant mole fractions). Here we provide only a summary of the necessary statistical mechanics in the interest of brevity. In the grand canonical pore ensemble, which is representative of gate-opening materials, the relevant partition function is given by

$$\Xi(\beta, \mu_1, \mu_2, h, N_s) = \sum_{N_{\text{tot}}} \exp(\beta \mu_1 N_{\text{tot}}) \times \Upsilon(\beta, \Delta\mu_2, h, N_{\text{tot}}, N_s), \quad (3)$$

where  $N_{\text{tot}}$  is the total number of adsorbate molecules in the slit-pore ( $N_1 + N_2$ ),  $N_s$  refers to the fictitious number of atoms or molecules that comprise the slit-pore,  $\beta \equiv 1/k_B T$ , and  $\Upsilon$  is the isochoric semigrand partition function

$$\Upsilon(\beta, \Delta\mu_2, h, N_{\text{tot}}, N_s) = \sum_{N_2} \exp(\beta \Delta\mu_2 N_2) \times Q(\beta, h, N_2, N_{\text{tot}}, N_s), \quad (4)$$

where  $Q(\beta, h, N_2, N_{\text{tot}}, N_s)$  refers to the system’s canonical partition function. The total canonical partition function may be expressed as a product of the partition functions of the pure solid,  $Q_s$ , and the one which captures all fluid-fluid and fluid-pore interactions,  $Q_f$ , assuming they are independent of each other,

$$Q(\beta, h, N_2, N_{\text{tot}}, N_s) = Q_s(\beta, h, N_s) \times Q_f(\beta, h, N_2, N_{\text{tot}}, N_s). \quad (5)$$

During a WL-TMMC simulation, sampling occurs according to  $Q_f$  only. However, because of this assumption, we may impose the free energy of the empty SPC, *a posteriori*, according to

$$\ln Q_s(\beta, h, N_s) = -\beta F_s(h), \quad (6)$$

where  $F_s(h)$  is some free energy profile which varies as a function of the pore width. This  $F_s(h)$  function captures the flexibility of a material and may be arbitrarily imposed during the reconstruction of  $\ln \Pi(h, N_{\text{tot}})$ .<sup>15</sup> In the grand canonical pore ensemble,  $h$  corresponds to the dimensions of the pores not the SPC's macroscopic size, which is fixed. The osmotic pore ensemble, which characterizes breathing materials, corresponds to a fixed pressure. In this case,  $h$  refers to the material's macroscopic dimension, which fluctuates in this ensemble. See Ref. 15 for more details. The osmotic pore partition function is given by

$$\Gamma(\beta, \mu_1, \mu_2, P_{\text{tot}}, N_s) = \sum_h \exp(-\beta P_{\text{tot}} A h) \times \Xi(\beta, \mu_1, \mu_2, h, N_s), \quad (7)$$

where  $P_{\text{tot}}$  is the total pressure of the adsorbate-adsorbent system and  $A$  is the slit-pore's cross-sectional area. Once again, an arbitrary  $F_s(h)$  may be imposed. Hence, the logarithm of the probability of a given macrostate, defined by the pore width and total number of adsorbate particles, is known up to some additive constant,  $C$ , in each ensemble,

$$\ln \Pi_{\text{gc}}(h, N_{\text{tot}}) = \beta(-F_s(h) + \mu_1 N_{\text{tot}}) + C_{\text{gc}}, \quad (8)$$

$$\ln \Pi_{\text{os}}(h, N_{\text{tot}}) = \beta(-F_s(h) - P_{\text{tot}} A h + \mu_1 N_{\text{tot}}) + C_{\text{os}}. \quad (9)$$

These constants do not affect the thermodynamic properties of the system and are neglected in practice. In this work, we focus on macroscopically deformable materials, described by Eq. (9), as we impose additional mechanical pressure constraints. In previous work, the adsorbate reservoir and the SPC were considered to be in direct mechanical equilibrium,<sup>15,19</sup> thus  $P_{\text{tot}}$  was simply taken as the bulk adsorbate fluid's pressure. In that case,  $P_{\text{tot}}$  is a function of the temperature and chemical potentials of its components, such that  $P_{\text{tot}} = P_f(\beta, \mu_1, \mu_2)$ . However, here we consider two scenarios where the total pressure is not necessarily given by the pressure of the fluid reservoir.

In this first scenario, we apply an additional constant, uniform mechanical pressure,  $P_{\text{add}}$ , to the SPC such that

$$P_{\text{tot}} = P_f(\beta, \mu_1, \mu_2) + P_{\text{add}}. \quad (10)$$

Positive and negative values of  $P_{\text{add}}$  correspond to compressive and tensile forces, respectively. In the second scenario, we fix the value of  $P_{\text{tot}}$  by varying  $P_{\text{add}}$  in Eq. (10) as a function of  $P_f$ . Note that according to Eqs. (8) and (9), if  $P_{\text{tot}} = 0$  the two pore ensembles have identical joint probability distributions. More generally, if  $P_{\text{tot}}$  is held at any constant value, one may formally replace the free energy profile,  $F_s(h)$ , with an effective one which is the sum of the material's inherent chemistry and the volumetric work terms, graphically depicted in Fig. 1(b),

$$F_e(h) = F_s(h) + (PA)h \quad (11)$$

When  $P_{\text{tot}}$  is fixed,  $P = P_{\text{tot}}$  in Eq. (11) and the work term may be entirely combined with  $F_s(h)$  so that Eq. (9) appears structurally identical to Eq. (8) with a free energy profile given by  $F_e(h)$  instead; however, this is not possible when there is a fixed additive pressure,  $P = P_f(\beta, \mu_1, \mu_2) + P_{\text{add}}$ . This is because  $P$  is no longer independent of  $P_f$ , and  $F_s(h)$  can only

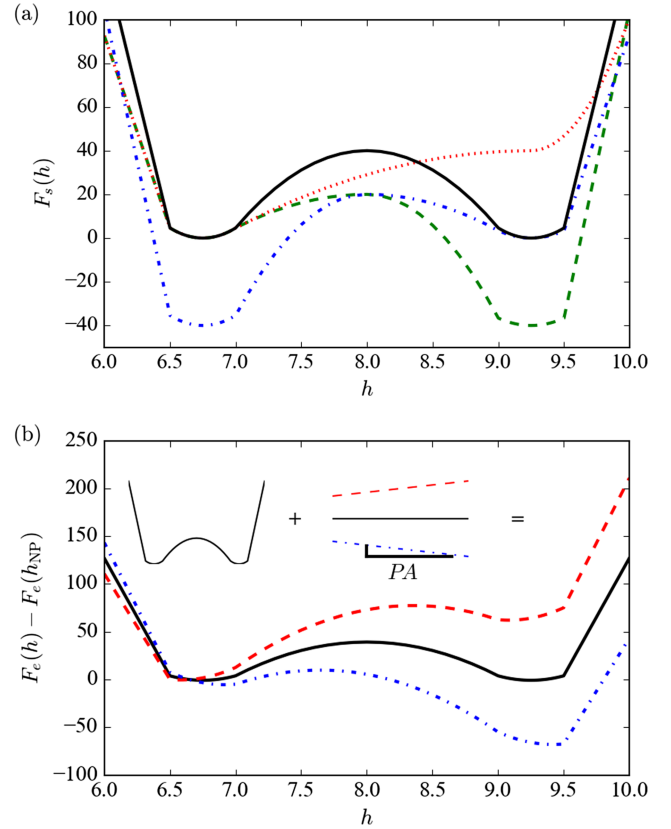


FIG. 1. (a) Bare SPC free energy profiles investigated here, each illustrated with different lines and colors for visual clarity. The NP phase is centered at a width of  $h_{\text{NP}} = 6.75\sigma_{2,2}$  and the LP phase at a width of  $h_{\text{LP}} = 9.25\sigma_{2,2}$ . (b) Schematic of the effective free energy profile that results from the sum of a profile from part (a) and an additional pressure,  $P$ , which is constant. The red curve corresponds to a compressive force, the blue to a tensile one, and the black to  $P = 0$ .

be transformed into an effective  $F_e(h)$  through the adoption of additional terms which are independent of the thermodynamic state of the adsorbate fluid.

Thus, for this model, there exists an analogy between the two ensembles when  $P_{\text{tot}}$  is held constant. Essentially, this implies that the thermodynamic description of a breathing material held at fixed overall pressure has a mathematical form identical to an unconstrained gate-opening material. Alternatively, it can be interpreted that by tuning  $P_{\text{tot}}$ , one can tune the effective free energy of the bare SPC. This is the basis for the following investigation. Formally, we point out that  $h$  corresponds to different dimensions (internal, accessible pore volume vs. macroscopic volume) in the different ensembles but are nonetheless related.<sup>15,19</sup>

Once the joint probability distribution has been constructed, it may be segmented into domains which define the NP and LP phases. A point in  $(h, N_{\text{tot}})$  space is assigned to a given phase by mapping it to local maxima in  $\ln \Pi(h, N_{\text{tot}})$ , following a path of steepest ascent.<sup>19</sup> For an empty SPC, the basin in  $F_s(h)$  located at the smaller pore width defines the NP phase, while the basin at the larger pore width corresponds to the LP phase. All extensive properties,  $X$ , of a phase,  $\alpha$ , may be calculated according to the following equation:

$$\langle X^\alpha \rangle = \sum_{(h, N_{\text{tot}}) \in \alpha} \tilde{\Pi}(h, N_{\text{tot}}) X(h, N_{\text{tot}}), \quad (12)$$

where the macrostate distribution has been normalized such that

$$\sum_h \sum_{N_{\text{tot}}} \tilde{\Pi}(h, N_{\text{tot}}) = 1. \quad (13)$$

The selectivity of a material,  $S_{1,2}$ , is defined as

$$S_{1,2} = \frac{x_{1,\text{ads}}/x_{1,\text{bulk}}}{x_{2,\text{ads}}/x_{2,\text{bulk}}}, \quad (14)$$

where  $x_i = \langle N_i \rangle / (\langle N_1 \rangle + \langle N_2 \rangle)$  is the mole fraction of species  $i$  in the bulk or adsorbed in the pore. The corresponding free energies are known up to some constant which is the product of the empty SPC's chemical potential,  $\mu_s^0$ , and  $N_s$  (Gibbs free energy)<sup>11,19</sup>

$$\beta(\Psi^\alpha - \mu_s^0 N_s) = \ln \left( \sum_h \tilde{\Pi}_{\text{os}}(h, 0) \right) - \ln \left( \sum_{(h, N_{\text{tot}}) \in \alpha} \tilde{\Pi}_{\text{os}}(h, N_{\text{tot}}) \right). \quad (15)$$

We also assess the properties of the ‘‘overall’’ material, in which case we compute thermodynamic properties on the basis of the entire macrostate distribution, without any segmentation. Although for our system we have considered only a single pore, mathematically, this formalism is identical to the case of a monolithic adsorbent composed of many individual pores. In this case, all pores deform collectively such that the probability of each macrostate refers to the chance of instantaneously observing the material collectively in that state. Alternatively, one may view this result as a representative of an adsorbent composed of an ensemble of independent pores, each existing in different polymorphic forms according to their relative probabilities, determined by their relative free energies. Regardless, this ‘‘average’’ result serves as a guide to the eye which helps to easily identify the thermodynamically stable polymorph.

### III. RESULTS AND DISCUSSION

For the supercritical binary fluid described in Table I, we investigated the effects of external barostatting via both a constant additive pressure and by holding the overall pressure of

the SPC fixed. We have done this for all fluid-wall interactions and  $F_s(h)$  profiles described in Table II and Fig. 1(a), respectively. The fluid-wall interactions determine the shape of the material's selectivity and other properties as described in Refs. 15 and 19. However, we found that the changes resulting from the externally applied pressure do not depend on these details. Consequently, we explicitly present only the results for Case I in Table II which are representative.

As a baseline, we summarize the relevant conclusions of previous work.<sup>15,19</sup> The binary supercritical fluid we employ here as a model adsorbate is size-asymmetric, where species 1 is larger than species 2. The fluid-wall interaction range for species 1 is also longer than that of species 2 ( $\lambda_{1,1}\sigma_{1,1} > \lambda_{2,2}\sigma_{2,2}$ ). Thus, even though the fluid-wall interaction strength is identical for both species in Case I, species 1 is adsorbed slightly more favorably than species 2 at low pressure. As the pressure of the fluid reservoir,  $P_f$ , increases, the smaller species becomes more entropically favored leading to a decrease in  $S_{1,2}$  for both the NP and LP phases. For the same reason, the LP phase tends to be more selective for the larger component than the NP phase; consequently, during the adsorption process their  $S_{1,2}$  curves appear qualitatively similar but are shifted relative to each other (cf., Fig. 2). These conclusions tend to hold generally, though for a material with a certain  $F_s(h)$  profile the precise behavior of  $S_{1,2}$  depends on the parameters in Table II.<sup>15</sup> These parameters also set the range over which a polymorph remains metastable, which determines the nature of hysteresis during adsorption-desorption cycles;<sup>19</sup> the limit of stability is defined as the point at which local maxima in  $\ln \Pi(h, N_{\text{tot}})$  (minima in free energy) merge with the curve dividing the two phases to create a saddle point. Here we report the thermodynamic properties of a polymorph over the range of pressures where it is either stable or metastable.

#### A. Additive pressure

In Fig. 2 we present the adsorption behavior of a flexible slit-pore in the osmotic pore ensemble when a constant additive pressure has been applied. We consider three bulk adsorbate fluids at different fixed compositions. For a SPC with the  $F_s(h)$  used in this case (blue curve of Fig. 1(a)), the NP polymorph

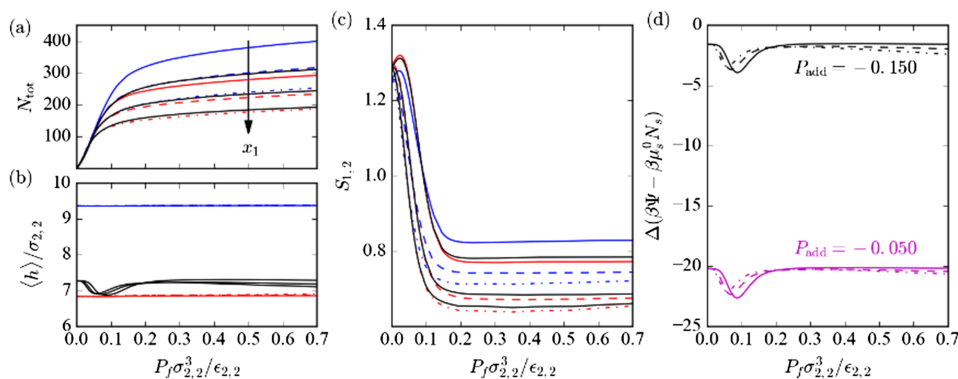


FIG. 2. Adsorption behavior of the SPC (Case I) when  $F_s(h)$  is given by the blue curve in Fig. 1(a) and a constant additive pressure has been applied. Here, red curves correspond to the NP phase and blue to the LP. Throughout, solid, dashed, and dot-dashed lines correspond to bulk fluid mole fractions of  $x_1 = 0.25, 0.50, 0.75$ , respectively. In ((a)–(c))  $P_{\text{add}} = -0.150$  and the material's overall behavior is depicted by solid black curves for each  $x_1$ . (a) The total number of adsorbed molecules,  $N_{\text{tot}}$ , (b) pore width,  $\langle h \rangle$ , (c) selectivity of the material, and (d) difference in free energy between the two phases over their mutual range of existence. The magenta curve in (d) depicts the result of a smaller  $P_{\text{add}}$  than the black curve at which ((a)–(c)) are reported.

is more more stable than the LP when no adsorbate is present. Therefore, when no external pressure is placed on the SPC during adsorption, the NP phase tends to remain more stable than the LP and the overall behavior of the material is essentially identical to that of the NP (red curves in Fig. 2). However, when  $P_{\text{add}}$  becomes sufficiently negative (tension), the difference in free energy between the two polymorphs approaches zero. As this happens, the average pore width, adsorption isotherms, and selectivity of the material become an average of the two phases. In Fig. 2 the applied tension is insufficient to stabilize the LP phase; however, if this tension is increased further, the LP phase may be stabilized, or the SPC may exhibit multiple equilibrium pressures between the polymorphs (cf., Fig. 3).

This is a consequence of the innate ‘‘dip’’ in the free energy difference between the polymorphs at  $P_f \sigma_{2,2}^3 / \epsilon_{2,2} \approx 0.1$ , which also notably manifests in  $\langle h \rangle$ . Breathing materials exhibit this signature in which a small amount of adsorbate applies a compressive force on the material favoring the collapsed form of the SPC. The compressive force results from adsorbate molecules interacting with opposite pore walls simultaneously, thus producing an indirect attraction between them. The difference in free energies in Fig. 2 and all subsequent figures is defined such that when  $\Delta(\beta\Psi - \beta\mu_s^0 N_s) < 0$  the NP phase has a lower free energy (more thermodynamically stable) than the LP phase. Thus, the dip reflects the further stabilization of the NP polymorph.

Breathing SPCs are named for their ability to undergo a LP  $\rightarrow$  NP  $\rightarrow$  LP transition as adsorbate pressure increases. In such a case,  $\Delta(\beta\Psi - \beta\mu_s^0 N_s)$  is positive at low adsorbate loading, becomes negative as adsorbate pressure increases, then becomes positive again at higher pressure due to entropic packing considerations in the pore. It is clear how the non-monotonic shape of  $\Delta(\beta\Psi - \beta\mu_s^0 N_s)$  as a function of pressure in Fig. 2 makes this possible when sufficient tension is applied. The general shape of this curve is characteristic of many fluid-wall interaction parameters; however, under certain circumstances, multiple breathing transitions are also theoretically possible.<sup>19</sup> We note that although  $\Delta(\beta\Psi - \beta\mu_s^0 N_s)$  may cross zero, hysteresis may prevent these transitions from being observed experimentally, as kinetic effects are known to affect the pressures at which these transitions are observed.<sup>22</sup> Capillary phase transitions during fluid adsorption tend to occur closer to the thermodynamic limit of stability of the phase in which the pore begins, whereas they tend to occur at the equilibrium phase coexistence point during desorption. For the specific instance we have considered here, hysteresis is

expected to be pronounced as the two SPC polymorphs remain at least metastable over a large range of adsorbate pressures. However, it is known that appropriately tuning the relative difference between the well depths in  $F_s(h)$  or the activation barrier between the two polymorphs can minimize this effect by entirely destabilizing a polymorph.<sup>19</sup> An example of this will be considered in Sec. III B.

In Figs. 2 and 3, we have only considered the case where the NP phase is thermodynamically more stable than the LP in the absence of any adsorbate. Conversely, when the LP phase is more stable (green curve in Fig. 1(a)), a positive  $P_{\text{add}}$  can accomplish a similar effect that tension can in these figures. In that case, the  $\Delta(\beta\Psi - \beta\mu_s^0 N_s)$  curves have a similar shape but are positive rather than negative in the absence of imposed pressure. In fact, regardless of  $F_s(h)$ , we find that when a constant additive pressure is imposed,  $\Delta(\beta\Psi - \beta\mu_s^0 N_s)$  is linearly shifted in accordance with the sign of  $P_{\text{add}}$ . Hence, for the additional cases when  $F_s(h)$  is given by either the red or black curves in Fig. 1(a), the corresponding  $\Delta(\beta\Psi - \beta\mu_s^0 N_s)$  curves for any  $P_{\text{add}}$  may be qualitatively obtained by shifting those corresponding to  $P_{\text{add}} = 0$  in the positive (negative) direction when  $P_{\text{add}}$  is negative (positive). These zero pressure curves have already been reported elsewhere.<sup>19</sup> Again, we emphasize these trends were found to be independent of the fluid-wall interactions we investigated and are equally valid for all cases in Table II.

## B. Fixed pressure

Next we contrast these results with the case when a breathing SPC is kept under constant overall pressure. Recall that this is mathematically analogous to exchanging this breathing material, described by some  $F_s(h)$ , for a gate-opening SPC characterized by some equivalent  $F_e(h)$  (cf., Fig. 1(b)). For all the different fluid-pore interactions described in Table II, we observed the same qualitative changes to the adsorption scenario relative to the case when the SPC was not barostat. First and foremost, the  $\Delta(\beta\Psi - \beta\mu_s^0 N_s)$  curve takes on a qualitatively different shape than before. Instead of the characteristic non-monotonicity observed traditionally in breathing materials, the curve becomes essentially monotonic and linear, which is characteristic of gate-opening SPCs<sup>19</sup> and is a direct consequence of this analogy.

Consider the case when  $F_s(h)$  is given by the black curve in Fig. 1(a). As shown previously,<sup>19</sup> in the absence of any external barostat, a gate-opening SPC with such a free energy profile exhibits phase coexistence between its polymorphs when

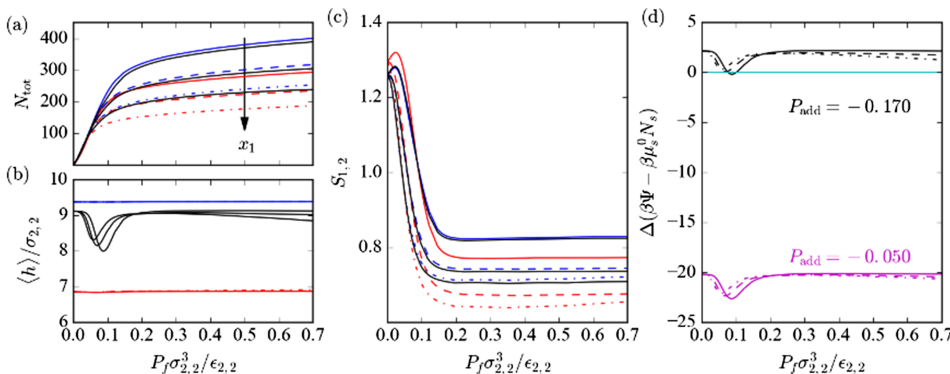


FIG. 3. Adsorption behavior of the SPC (Case I) at conditions reported in Fig. 2. Here we illustrate the effects when the SPC is under slightly more tension,  $P_{\text{add}} = -0.170$ , than shown in Fig. 2. The curves for  $P_{\text{add}} = -0.050$  in (d) are added simply for reference.

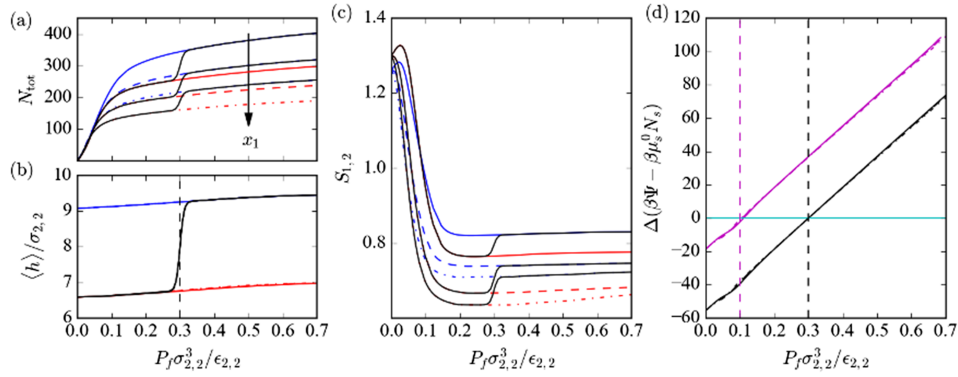


FIG. 4. Adsorption behavior of the SPC (Case I) when  $F_s(h)$  is given by the black curve in Fig. 1(a) and the total pressure exerted on the SPC has been fixed. Here, red curves correspond to the NP phase and blue to the LP. Throughout, solid, dashed, and dot-dashed lines correspond to  $x_1 = 0.25, 0.50, 0.75$ , respectively. In ((a)–(c)) the material’s overall behavior is depicted by solid black curves for clarity. (a) The total number of adsorbed molecules,  $N_{\text{tot}}$ , (b) pore width,  $\langle h \rangle$ , (c) selectivity of the material, and (d) difference in free energy between the two phases over their mutual range of existence. The magenta curve in (d) depicts the result for  $P_{\text{tot}}\sigma_{2,2}^3/\epsilon_{2,2} = 0.10$ , whereas the black curve corresponds to  $P_{\text{tot}}\sigma_{2,2}^3/\epsilon_{2,2} = 0.30$  at which ((a)–(c)) are reported. These values are indicated by vertical dashed lines.

empty. However, as fluid adsorbs, the LP phase immediately becomes stabilized over the NP polymorph. Compare this with the case when the overall pressure on a breathing material with the same  $F_s(h)$  is fixed at  $P_{\text{tot}}\sigma_{2,2}^3/\epsilon_{2,2} = 0.30$ , as illustrated in Fig. 4. In fact, this is precisely the behavior we observe in the barostatted breathing SPC; however, the stabilization of the LP polymorph occurs when the adsorbate fluid pressure reaches that of the barostat, rather than beginning at zero pressure. Below the barostat pressure, the NP phase is stable because the barostat is applying a compressive force on the adsorbent. Indeed, when any barostat is applied to this breathing SPC to fix its overall pressure, we found that the result is a simple shift of the transition pressure from  $P_f\sigma_{2,2}^3/\epsilon_{2,2} = 0$  to  $P_{\text{tot}}$ . The overall SPC’s equilibrium adsorption isotherm, selectivity, and average pore size clearly reflect this change in the relative stability of the polymorphs. Thus, the thermodynamic behavior of a macroscopically flexible, breathing SPC is essentially transformed into that of a macroscopically rigid, gate-opening material, whose effective gate-opening pressure is determined by  $P_{\text{tot}}$ . This does not imply that a breathing SPC does not macroscopically deform under these conditions, rather that this deformation has qualitatively different consequences on the thermodynamic behavior of the SPC.

One may graphically summarize the effect of barostatting a breathing SPC as follows. When barostatting to different fixed additive pressures, the  $\Delta(\beta\Psi - \beta\mu_s N_s^0)$  vs.  $P_f$  curves of

the SPC are shifted “vertically.” By contrast, when a barostat is employed to fix the overall pressure of the SPC throughout the adsorption process, these curves are transformed into those of gate-opening materials and subsequently shifted “horizontally” by the magnitude of the barostat. To further illustrate this point, consider the case where the SPC’s inherent free energy profile is given by the red curve in Fig. 1(a). For this material, the NP phase is clearly stable in the absence of adsorbate fluid. Its  $F_s(h)$  curve also has an inflection point at larger  $h$ , which may become a stable LP phase at higher pressures. In Fig. 5, we present results for this SPC under a fixed pressure of  $P_{\text{tot}}\sigma_{2,2}^3/\epsilon_{2,2} = 0.30$ . When  $P_f < P_{\text{tot}}$  there is an external compressive force applied to the material, whereas when  $P_f > P_{\text{tot}}$  some amount of external tension is applied. The SPC remains in the NP phase during initial fluid adsorption and is the only stable phase present. Eventually, the LP phase appears as a metastable branch before the equilibrium NP  $\rightarrow$  LP transition occurs. Beyond this transition pressure, the NP phases eventually lose stability at sufficiently high  $P_f\sigma_{2,2}^3/\epsilon_{2,2}$ . The vertical black dashed line in Fig. 5(b) indicates  $P_{\text{tot}}$  for reference but represents the origin in the case when no external pressure is applied (cf., Ref. 19).

Similarly, in the case where the LP phase is the most stable form in the limit of  $P_f\sigma_{2,2}^3/\epsilon_{2,2} \rightarrow 0$  (green curve in Fig. 1(a)), a positive (compressive) pressure will stabilize the NP as expected. Figure 6 shows the result; in the absence of any external pressure, the LP is initially the most stable phase

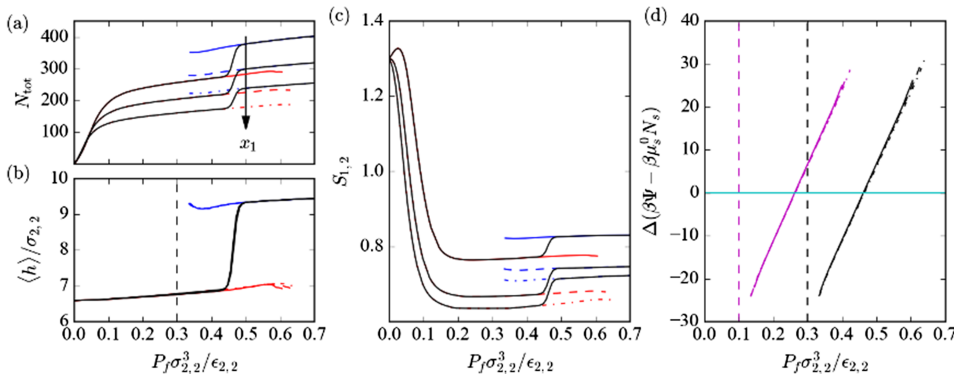


FIG. 5. Adsorption behavior of the SPC (Case I) when  $F_s(h)$  is given by the red curve in Fig. 1(a) and the total pressure exerted on the SPC has been fixed. Symbols and curves are described in Fig. 4.

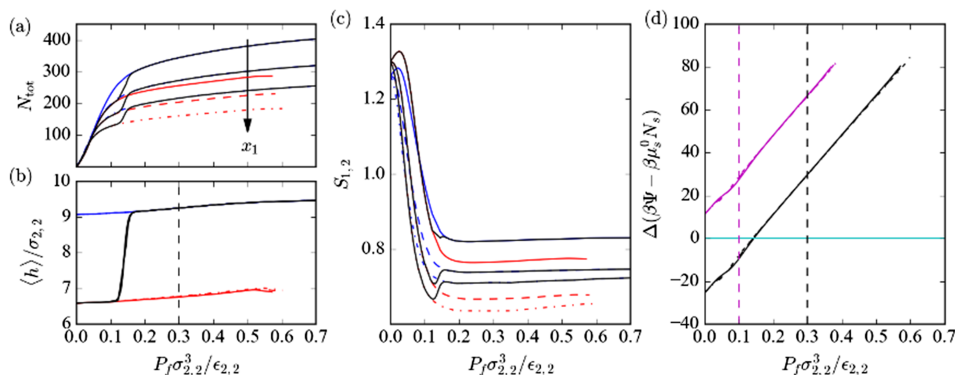


FIG. 6. Adsorption behavior of the SPC (Case I) when  $F_s(h)$  is given by the green curve in Fig. 1(a) and the total pressure exerted on the SPC has been fixed. Symbols and curves are described in Fig. 4.

and remains so over the complete course of adsorption and desorption. However, if sufficient tension is applied, the NP is stabilized for low  $P_f \sigma_{2,2}^3 / \epsilon_{2,2}$ .

Therefore, by fixing the overall pressure of the material, the equilibrium transition point between the SPC polymorphs can be shifted. Note that this horizontal shift of the  $\Delta(\beta\Psi - \beta\mu_s N_s^0)$  curve leaves the extent of the metastability (hysteresis window) relatively unaffected for most of the specific  $F_s(h)$  profiles we have considered here. For example, only a very weak change in the length of the black vs. magenta curves in Fig. 5(d) appears. However, if  $F_s(h)$  has either a smaller activation free energy barrier or difference between the well depths corresponding to its polymorphs, then it is conceivable that a linear “PV” addition may produce more pronounced changes to the range of pressures over which the two phases are metastable. Using macroscopic elastic theory, the broadening of this range of metastability over which adsorption-desorption hysteresis may be observed has been predicted for certain elastic core-shell or mixed-membranes containing SPCs.<sup>20</sup> Our simulations agree with this qualitative prediction and illustrate how this is a consequence of a SPC’s  $F_s(h)$  profile being effectively modified by the externally applied pressure. Quantitatively, the extent of this effect will depend on the exact nature of  $F_s(h)$  and the geometry of the SPC, which here has been simplified to a slit-pore.

#### IV. CONCLUSIONS

We considered the thermodynamic behavior of polymorphic soft porous crystals which may “breathe” in response to applied stress, when additional external pressure is applied. Specifically, we investigated two different barostatting scenarios. In the first, when a constant pressure is applied to the SPC in addition to the thermodynamic pressure of the adsorbate, the free energy difference between the SPC’s polymorphs shifts to higher or lower values depending on the sign of  $P_{\text{add}}$ . This allows the relative stability of the two polymorphs to be controlled through external barometric means. Since the overall properties of the SPC reflect those of its most stable polymorph, characteristics of the adsorbent, such as its selectivity, may be tuned as a consequence.

In the second scenario, where a breathing SPC is held at fixed overall pressure, there is a direct analogy between the mathematical form describing the statistical mechanics of this material and a gate-opening one. We illustrated how breathing

SPCs with a certain inherent free energy profile are thermodynamically equivalent to gate-opening SPCs with a different profile that has been modified by a volumetric work correction. The result is that the curve describing the free energy difference between the barostatted breathing SPC’s polymorphs is transformed into one describing an equivalent non-barostatted gate-opening material, which is subsequently shifted by the magnitude of the barostat. This demonstrates that one can effectively fine tune the free energy profile of a SPC simply by imposing a fixed pressure on the material, whereas conventional wisdom is to achieve this by modifying the chemistry of its ligands and metal centers. We expect these conclusions to encourage experimental work developing hybrid adsorbents, such as core-shell SPC composites,<sup>20</sup> which can plausibly realize such barostats.

#### ACKNOWLEDGMENTS

Contribution of the National Institute of Standards and Technology, not subject to US Copyright. N.A.M. gratefully acknowledges support from a National Research Council post-doctoral research associateship at the National Institute of Standards and Technology.

<sup>1</sup>K. Uemura, R. Matsuda, and S. Kitagawa, “Flexible microporous coordination polymers,” *J. Solid State Chem.* **178**(8), 2420–2429 (2005).

<sup>2</sup>S. Horike, S. Shimomura, and S. Kitagawa, “Soft porous crystals,” *Nat. Chem.* **1**(9), 695–704 (2009).

<sup>3</sup>F.-X. Coudert, A. Boutin, A. H. Fuchs, and A. V. Neimark, “Adsorption deformation and structural transitions in metal-organic frameworks: From the unit cell to the crystal,” *J. Phys. Chem. Lett.* **4**, 3198–3205 (2013).

<sup>4</sup>H. Furukawa, K. E. Cordova, M. O’Keefe, and O. M. Yaghi, “The chemistry and applications of metal-organic frameworks,” *Science* **341**, 123044 (2013).

<sup>5</sup>D. Fairen-Jimenez, S. A. Moggach, M. T. Wharmby, P. A. Wright, S. Parsons, and T. Düren, “Opening the gate: Framework flexibility in ZIF-8 explored by experiments and simulations,” *J. Am. Chem. Soc.* **133**, 8900–8902 (2011).

<sup>6</sup>L. Zhang, Z. Hu, and J. Jiang, “Sorptions-induced structural transitions of zeolitic imidazolate framework-8: A hybrid molecular simulation study,” *J. Am. Chem. Soc.* **135**, 3722–3728 (2013).

<sup>7</sup>A. V. Neimark, F.-X. Coudert, A. Boutin, and A. H. Fuchs, “Stress-based model for the breathing of metal-organic frameworks,” *J. Phys. Chem. Lett.* **1**, 445–449 (2010).

<sup>8</sup>A. Ghysels, L. Vanduyfhuys, M. Vandichel, and M. Waroquier, “On the thermodynamics of framework breathing: A free energy model for gas adsorption in MIL-53,” *J. Phys. Chem. C* **117**, 11540–11554 (2013).

<sup>9</sup>J. A. Mason, J. Oktawiec, T. K. Mercedes, M. R. Hudson, J. Rodriguez, J. E. Bachman, M. I. Gonzalez, A. Cervellino, A. Guagliardi, C. M. Brown, P. L. Llewellyn, N. Masciocchi, and J. R. Long, “Methane storage in flexible

- metal-organic frameworks with intrinsic thermal management,” *Nature* **527**, 357–361 (2015).
- <sup>10</sup>J. Wieme, L. Vanduyfhuys, S. M. J. Rogge, M. Waroquier, and V. V. Van Speybroek, “Exploring the flexibility of MIL-47(V)-type materials using force field molecular dynamics simulations,” *J. Phys. Chem. C* **120**, 14934 (2016).
- <sup>11</sup>V. K. Shen and D. W. Siderius, “Elucidating the effects of adsorbent flexibility on fluid adsorption using simple models and flat-histogram sampling methods,” *J. Chem. Phys.* **140**, 244106 (2014).
- <sup>12</sup>D. Britt, H. Furukawa, B. Wang, T. G. Glover, and O. M. Yaghi, “Highly efficient separation of carbon dioxide by a metal-organic framework replete with open metal sites,” *Proc. Natl. Acad. Sci. U. S. A.* **106**, 20637–20640 (2009).
- <sup>13</sup>F.-X. Coudert, “The osmotic framework adsorbed solution theory: Predicting mixture coadsorption in flexible materials,” *Phys. Chem. Chem. Phys.* **12**, 10904–10913 (2010).
- <sup>14</sup>M. Hartmann, U. Boehme, M. Hovestadt, and C. Paula, “Adsorptive separation of olefin/paraffin mixtures with ZIF-4,” *Langmuir* **31**, 12382 (2015).
- <sup>15</sup>N. A. Mahynski and V. K. Shen, “Multicomponent adsorption in mesoporous flexible materials with flat-histogram Monte Carlo methods,” *J. Chem. Phys.* **145**, 174709 (2016).
- <sup>16</sup>D. I. Fried, F. J. Brieler, and M. Fröba, “Designing inorganic porous materials for enzyme adsorption and applications in biocatalysis,” *ChemCatChem* **5**, 862–884 (2013).
- <sup>17</sup>P. Horcajada, C. Serre, G. Maurin, N. A. Ramsahye, F. Balas, M. Vallet-Regí, M. Sebban, F. Taulelle, and G. Férey, “Flexible porous metal-organic frameworks for a controlled drug delivery,” *J. Am. Chem. Soc.* **130**, 6774–6780 (2008).
- <sup>18</sup>A. U. Ortiz, M.-A. Springuel-Huet, F.-X. Coudert, A. H. Fuchs, and A. Boutin, “Predicting mixture coadsorption in soft porous crystals: Experimental and theoretical study of CO<sub>2</sub>/CH<sub>4</sub> in MIL-53(Al),” *Langmuir* **28**, 494–498 (2012).
- <sup>19</sup>N. A. Mahynski and V. K. Shen, “Tuning flexibility to control selectivity in soft porous crystals,” *J. Chem. Phys.* **146**, 044706 (2017).
- <sup>20</sup>F.-X. Coudert, A. H. Fuchs, and A. V. Neimark, “Adsorption deformation of microporous composites,” *Dalton Trans.* **45**, 4136–4140 (2016).
- <sup>21</sup>D. Bousquet, F.-X. Coudert, and A. Boutin, “Free energy landscapes for the thermodynamic understanding of adsorption-induced deformations and structural transitions in porous materials,” *J. Chem. Phys.* **137**, 044118 (2012).
- <sup>22</sup>T. Hiratsuka, H. Tanaka, and M. T. Miyahara, “Mechanism of kinetically controlled capillary condensation in nanopores: A combined experimental and Monte Carlo approach,” *ACS Nano* **11**, 269 (2016).